DMD Fast Forward. Published on June 19, 2020 as DOI: 10.1124/dmd.120.000061
This article has not been copyedited and formatted. The final version may differ from this version.

Dexamethasone-induced liver enlargement is related to PXR/YAP activation and lipid accumulation but not hepatocyte proliferation

Tingying Jiao[1#], Xinpeng Yao[1#], Yingyuan Zhao[1], Yanying Zhou[1], Yue Gao[1], Shicheng Fan[1], Panpan Chen[1], Xuan Li[1], Yiming Jiang[1], Xiao Yang[1], Frank J. Gonzalez[2], Min Huang[1], Huichang Bi[1*]

[1]Guangdong Provincial Key Laboratory of New Drug Design and Evaluation, School of Pharmaceutical Sciences, Sun Yat-sen University, Guangzhou, China, 510006

[2]Laboratory of Metabolism, Center for Cancer Research, National Cancer Institute, NIH, Bethesda, MD 20892, USA

[#]These two authors contributed equally to the work.

DMD Fast Forward. Published on June 19, 2020 as DOI: 10.1124/dmd.120.000061
This article has not been copyedited and formatted. The final version may differ from this version.

Running Title: PXR and YAP are involved in Dex-induced hepatomegaly

[*]**Correspondence to:** Huichang Bi, Ph.D. School of Pharmaceutical Sciences, Sun Yat-sen University, 132# Waihuandong Road, Guangzhou University City, Guangzhou 510006, P. R. China. Email: bihchang@mail.sysu.edu.cn. Phone: +86-20-39943470. Fax: +86-20-39943000

The number of text pages: 44

The number of figures: 5

The number of references: 61

The number of words in the *Abstract*: 246

The number of words in the *Introduction*: 577

The number of words in the *Discussion*: 1625

DMD Fast Forward. Published on June 19, 2020 as DOI: 10.1124/dmd.120.000061
This article has not been copyedited and formatted. The final version may differ from this version.

Abbreviations

ATGL/PNPLA2: adipose triglyceride lipase; ANKRD1: ankyrin repeat domain 1; CPT1A: carnitine palmitoyltransferase 1A; CCNA1: cyclin A1; CCND1: cyclin D1; CCNE1: cyclin E1; CTGF: connective tissue growth factor; CV: central vein; CYP: cytochrome P450; CYR61: cysteine-rich angiogenic inducer 61; DAPI: 4′, 6-diamidino-2-phenylindole; Dex: dexamethasone; DG: diacylglycerol; DGAT: diacylglycerol acyltransferase; ECL: electro-chemiluminescence; EGFR: epidermal growth factor receptor; FDR: false discovery rate; FOX: forkhead box protein; GR: glucocorticoids receptor; H&E: hematoxylin and eosin; HMGCS2: 3-hydroxy-3-methylglutarate-CoA synthase 2; hPXR: human PXR; HSL/LIPE: hormone-sensitive lipase; IgG: immunoglobulin G; IHC: immunohistochemistry; IL6: interleukin 6; Ifng: interferon γ; LST: liver-specific organic anion transporter; MET: mesenchymal-epithelial transition factor; MG: monoglycerides; MKP-3: MAP kinase phosphatase 3; mPXR: mouse PXR; NAFLD: non-alcoholic fatty liver disease; OATP: organic anion transporter polypeptide; OCT: optimal cutting temperature compound; OPLS-DA: orthogonal partial least squares discriminant analysis; PC: phosphatidylcholine; PCA: principal component analysis; PCN: pegnenolone-16α-carbonitrile; PCNA: proliferating cell nuclear antigen; PE: phosphatidyl ethanolamine; PI: phosphatidylinositol; PV: portal vein; PXR: pregnane X receptor; p-YAP: phosphorylated YAP; RIF: rifampicin; RTKs: receptor tyrosine kinases; SLC: solute carrier family; SLCO: solute carrier organic anion transporter family; TG:

DMD Fast Forward. Published on June 19, 2020 as DOI: 10.1124/dmd.120.000061
This article has not been copyedited and formatted. The final version may differ from this version.

triglyceride; TNF: tumor necrosis factor; UHPLC-ESI-HRMS: ultra-high-performance liquid chromatography coupled with electrospray ionization high-resolution mass spectrometry; VIP: variable importance in projection; YAP: yes-associated protein.

DMD Fast Forward. Published on June 19, 2020 as DOI: 10.1124/dmd.120.000061
This article has not been copyedited and formatted. The final version may differ from this version.

ABSTRACT

Dexamethasone (Dex), a widely prescribed anti-inflammatory drug, was reported to induce liver enlargement (hepatomegaly) in clinical practice and in animal models. However, the underlying mechanisms are not elucidated. Dex is a known activator of pregnane X receptor (PXR). Yes-associated protein (YAP) has been implicated in chemically-induced liver enlargement. Here the roles of PXR and YAP pathways were investigated in Dex-induced hepatomegaly. Upregulation of PXR downstream proteins including CYP3A11, CYP2B10 and OATP2 (also known as SLCO1A4 and SLC21A5 in mouse) is indicated PXR signaling was activated after high dose of Dex (50 mg/kg, *i.p.*), and Dex at 100 μM activated PXR in the dual-luciferase reporter gene assay. Dex also increased the expression of total YAP, nuclear YAP, and YAP downstream proteins including CTGF and CYR61, indicating activation of the YAP pathway. Furthermore, nuclear translocation of YAP was promoted by activation of PXR. However, hepatocyte proliferation was inhibited with significant decrease in the expression of proliferation-related proteins CCND1 and PCNA, as well as other regulatory factors, such as FOXM1, c-MYC and EGFR. The inhibitory effect of Dex on hepatocyte proliferation was likely due to its anti-inflammation effect of suppression of inflammation factors. CTNNB1 staining revealed enlarged hepatocytes which were mostly attributable to the accumulation of lipids such as triglycerides. In summary, high-dose Dex increased liver size accompanied by enlarged hepatocytes, due to the activation of PXR/YAP and their effects on lipid accumulation, but not hepatocyte proliferation. These findings provide new insights for understanding the mechanism of Dex-induced hepatomegaly.

DMD Fast Forward. Published on June 19, 2020 as DOI: 10.1124/dmd.120.000061
This article has not been copyedited and formatted. The final version may differ from this version.

Keywords

Dexamethasone (Dex); liver enlargement; hepatomegaly; pregnane X receptor (PXR); yes-associated protein (YAP).

Significance Statement

- This study identified the roles of PXR and YAP pathways in Dex-induced hepatomegaly. Dex induced PXR/YAP activation, enlarged hepatocytes and promoted liver enlargement with lipid accumulation such as triglycerides. However, hepatocyte proliferation was inhibited by the anti-inflammatory effect of Dex. These findings provide new insights for understanding the mechanism of Dex-induced hepatomegaly.

DMD Fast Forward. Published on June 19, 2020 as DOI: 10.1124/dmd.120.000061
This article has not been copyedited and formatted. The final version may differ from this version.

Introduction

Dexamethasone (16α-methyl 9α-fluoroprednisolone, Dex) is a synthetic glucocorticoid. Owing to its potency for anti-inflammation, Dex has been widely applied in clinic for decades as a treatment for diverse inflammatory and autoimmune diseases, e.g. rheumatic arthritis, asthma, allergy and transplantation rejection (Ericson-Neilsen and Kaye 2014; Rhen and Cidlowski 2005). Dex also has an influence on the physiological process of metabolism of endogenous compounds including lipids (Harasim-Symbor et al. 2016), glucose (Cui et al. 2019) and bile acids (Glantz et al. 2005). Most of the physiological effects of Dex are mediated through the glucocorticoid receptor (GR), a member of the nuclear receptor superfamily of transcription factors (Petta et al. 2016). Apart from GR, Dex is also an agonist of the nuclear receptor pregnane X receptor (PXR) and can induce specific drug metabolizing enzymes such as the cytochrome P450 enzyme (CYP) 3A4 (Buckley and Klaassen 2009; Cheng et al. 2005). Different dose and frequency of Dex treatment can lead to various side effects, which may be due to activation of GR or PXR. It was reported that high-dose Dex treatment induced hepatomegaly accompanied by increased glycogen and lipids contents in clinical cases (Verrips et al. 1998). Consistently, a similar phenomenon was observed in animal models (Micuda et al. 2007; Thatcher and Caldwell 1994). However, the related mechanisms of the Dex-induced hepatomegaly remain unknown and need to be clarified.

DMD Fast Forward. Published on June 19, 2020 as DOI: 10.1124/dmd.120.000061
This article has not been copyedited and formatted. The final version may differ from this version.

In mammals, the liver plays a crucial role in xenobiotic metabolism including drugs and chemicals, which puts an emphasis on maintaining a constant liver mass and size. As a rapid response system that is responsible for the stability of normal homeostasis and tight control of biological parameters, the liver regulates its size not only by genetic factors but by a range of stimuli, such as hormonal fluctuations during pregnancy and lactation, acute-phase proteins stimulated by infections by viruses and bacteria, and enzymes induced by xenobiotics (Botts et al. 2010). The response of the liver to these different stimuli may include an increase in the size and capacity of function of the liver due to an increase in the size and number of hepatocytes, which is also defined as hepatocyte hypertrophy and hepatocellular hyperplasia (Maronpot et al. 2010).

Due to the flexible pocket domain, PXR can bind to a variety of structurally-diverse ligands including steroids, bile acids and antibiotics such as rifampicin (RIF) (Kliewer et al. 2002). PXR is expressed in the liver and plays a vital role in controlling the transport and metabolism of xenobiotics, as well as maintaining the homeostasis of certain endobiotics (Kliewer et al. 1998; Xie et al. 2000). Pregnenolone-16α-carbonitrile (PCN), a PXR agonist, induced remarkable liver enlargement. Most recently, PXR was found to regulate liver size by interaction with yes-associated protein (YAP) (Jiang et al. 2019), indicating a critical role for YAP in the liver enlargement induced by PXR activation. YAP, the core component of Hippo-YAP pathway, plays an important role in controlling organ growth including the size of liver (Dong et al. 2007).

DMD Fast Forward. Published on June 19, 2020 as DOI: 10.1124/dmd.120.000061
This article has not been copyedited and formatted. The final version may differ from this version.

Hyperactivation of YAP can cause hepatomegaly with increased numbers of hepatocytes (Patel et al. 2017) A previous study also showed that high expression of YAP could result in potent cell enlargement (Tumaneng et al. 2012).

Based on the information mentioned above, we hypothesized that Dex-induced liver enlargement may be related to the activation of PXR and its interaction with YAP. Therefore, this study aimed to investigate whether PXR and YAP are involved in this process and explore the changes of lipids in Dex-induced hepatomegaly.

DMD Fast Forward. Published on June 19, 2020 as DOI: 10.1124/dmd.120.000061
This article has not been copyedited and formatted. The final version may differ from this version.

Materials and methods

Chemicals and reagents.

Dexamethasone (Dex) with 98% purity (Cat# D137736) and corn oil (Cat# C116025) were purchased from Aladdin Biotechnology (Aladdin Industrial Corporation, Shanghai, China). Rifampicin (RIF) with 97% purity (Cat# R3501) was acquired from Sigma Aldrich (Sigma, St. Louis, MO). Murine IL6 (Cat# 216-16-100) was obtained from PeproTech (Peprotech Inc, USA). Rabbit monoclonal anti-CCND1 (Cat# 2978T), anti-CCNE1 (Cat# 20808S), anti-PCNA (Cat# 13110S), anti-C-MYC (Cat# 13987S), anti-CTNNB1 (Cat# 8480S), anti-YAP (Cat# 14074S) and anti-β-actin (Cat# 4970S) antibodies were all obtained from Cell Signaling Technology (Cell Signaling Technology, MA, USA). Mouse monoclonal anti-CYP3A4 (Cat# sc-53850) antibody was purchased from Santa Cruz Biotechnology (Santa Cruz, CA, USA). Rabbit polyclonal anti-CYP2B6 (Cat# A1463) antibody was purchased from ABclonal Technology (Wuhan, China). Rabbit polyclonal anti-OATP2 (Cat# DF4534) antibody was obtained from Affinity Biosciences (Changzhou, China). Rabbit polyclonal anti-CCNA1 (Cat# D220507), anti-phosphorylated YAP (Cat# D151452), anti-ANKRD1 (Cat# D121628), anti-CYR61 (Cat# D122190), anti-CTGF (Cat# D160212), anti-EGFR (Cat# D260292), anti-MET (Cat# D160981) and anti-LMNB1 (Cat# D220926) antibodies were acquired from Sangon Biotechnology (Sangon Tech, Shanghai, China). Rabbit polyclonal anti-FOXM1 antibody (Cat# 13147-1-AP) was obtained from Proteintech (Proteintech Group, Inc, Wuhan,

DMD Fast Forward. Published on June 19, 2020 as DOI: 10.1124/dmd.120.000061
This article has not been copyedited and formatted. The final version may differ from this version.

China). Peroxidase-conjugated anti-rabbit immunoglobulin G (IgG) antibody (Cat# 7074S) and anti-mouse (Cat# 7076S) was purchased from Cell Signaling Technology. For the use of immunohistochemical staining, rabbit monoclonal Ki67 antibody (Cat# ab16667) was purchased from Abcam (USA) and purified mouse monoclonal CTNNB1 antibody (Cat# 610153) was from BD Biosciences (San Jose, CA). For the staining of co-location, rabbit polyclonal anti-PXR (Cat# sc-25381), and mouse monoclonal anti-YAP (Cat# MAB8094) were obtained from Santa Cruz and R&D Systems (MN, USA), respectively. 4′, 6-diamidino-2-phenylindole (DAPI) (Cat# C1002) was purchased from Beyotime Technology (Shanghai, China). Secondary antibodies including anti-rabbit IgG Alexa Fluor 647 (Cat# 4414S) and anti-mouse IgG Alexa Fluor 488 (Cat# 4408S) were from Cell Signaling Technology. The pSG5-hPXR expression vector was generously provided by Dr. Steven Kliewer (University of Texas Southwestern Medical Center, Dallas, TX, USA). The pGL3-CYP3A4-XREM luciferase reporter construct was generously provided by Dr. Jeff Staudinger (University of Kansas, Lawrence, KS, USA).

Experimental animals and treatments.

Adult male C57BL/6J mice (6-8 weeks old, 18-22 g) were purchased from Guangdong Medical Laboratory Animal Center. The animal room is specific-pathogen-free. Mice were housed under a standard 12 h light/12 h dark cycle and 55-60% humidity at 22-24°C with free access to water and a standard rodent chow. All animal experiments were operated in compliance

DMD Fast Forward. Published on June 19, 2020 as DOI: 10.1124/dmd.120.000061
This article has not been copyedited and formatted. The final version may differ from this version.

with the guidelines of the Institutional Animal Care and Use Committee of Sun Yat-sen University (Guangzhou, China).

For Dex treatment, all the mice were randomized to two groups. Dex at the dose of 50 mg/kg or corn oil (vehicle) at the dose of 0.1 mL/10 g was administered intraperitoneally (*i.p.*) once daily for 5 days. Livers were harvested at 24 h after the last injection. The body weight and liver weight of mice were both measured for calculation of liver-to-body-weight ratios. A portion of liver was rapidly fixed in 10% buffered formalin for histological examination. The rest of the tissues were immediately frozen by lipid nitrogen and stored at -80°C for further study.

Histological analysis.

Liver tissues were fixed in 10% buffered formalin solution. After being embedded in paraffin, specimens were cut into sections about 4 μm thick each. Sections were deparaffinized by different concentrations of xylene and ethyl alcohol and then stained with hematoxylin and eosin solutions (H&E, Servicebio, Wuhan, China). For immunohistochemical staining, paraffin-embedded sections were stained with primary antibodies against Ki67, PCNA and CTNNB1 after heat-induced epitope retrieval in citrate buffer. H&E staining and immunohistochemical staining were all visualized by an Olympus inverted microscope (Olympus IX73, Olympus Corporation, Japan).

Oil Red O staining.

DMD Fast Forward. Published on June 19, 2020 as DOI: 10.1124/dmd.120.000061
This article has not been copyedited and formatted. The final version may differ from this version.

The fixed liver tissue was removed from 10% buffered formalin solution to a 15% sucrose solution at 4°C for dewatering and sinking followed by a 30% sucrose solution. After coated with optimal cutting temperature compound (OCT) embedding agent, the section was cut into 10 μm thick after OCT turned white and hardened. The frozen sections were washed with PBS buffer and stained with oil red O working solution. Hematoxylin solutions was used to dye the nuclei.

Measurement of TG contents.

Triglyceride (TG) contents of liver tissue were measured by TG detection assay kits (Nanjing Jiancheng Bioengineering Institute, Nanjing, China). Generously, liver tissues were homogenized (weight of liver tissues: volume of PBS=1:9) and centrifuged at a speed of 2500 rpm for 10 min at 4°C. The procedure of TG contents analysis strictly followed the protocol that the manufacture provided. In brief, 2.5 μL distilled water, calibration solution (2.26 mmol/L TG solution) and sample tested were added to 250 μL working solution in 96-well plates respectively. After mixing and incubation at 37°C for 10 min, the absorbance of the mixture was measured at a wavelength of 500 nm. The calculation formula provided in the guidelines was applied for the analysis of hepatic total TG levels.

CCK8 test.

DMD Fast Forward. Published on June 19, 2020 as DOI: 10.1124/dmd.120.000061
This article has not been copyedited and formatted. The final version may differ from this version.

HEK293T cells (from ATCC) were cultured in DMEM containing 10% FBS (Gibco, USA) and 100 U penicillin/streptomycin. Cells were seeded into 96-well plates at 1×10^4 cells per well. After incubation overnight, the cells were treated with DMSO or Dex (6.25, 25, 100 and 400 μM) for 24 hours. Then 10 μL CCK8 (Dojindo laboratories, Shanghai, China) (Cat# CK04) was added to each well followed by two- to four-hour incubation. OD value was measured at a wavelength of 450 nm. This experiment was repeated three times independently.

Dual-luciferase reporter gene assays.

Dual-luciferase reporter gene assays were performed according to our previously reported protocols (Zeng et al. 2017). In general, HEK293T cells were seeded into 96-well plates at 1.2×10^4 cells per well and incubated overnight followed by the transfection of 100 ng pGL3-CYP3A4-XREM-Luc, 3 ng pGL4.54-TK and 50 ng pSG5-hPXR. The transfection processed according to Megatran 1.0 instructions (OriGene). The transfected mixture was replaced by serum-free medium Opti-MEM (Gibco, USA) 6 h later. Transfected cells were then treated with Dex (6.25, 25, 100 and 400 μM) and hPXR positive agonist RIF (10 μM) for 24 h. Luciferase activity was examined by a tube luminometer applied with the Dual Reporter Assay System (Berthold Technologies, Germany) following manufacturer's protocols. With Renilla activity as control, firefly luciferase activity was normalized to Renilla activity for each well.

HepG2 culture and immunofluorescence double staining.

DMD Fast Forward. Published on June 19, 2020 as DOI: 10.1124/dmd.120.000061
This article has not been copyedited and formatted. The final version may differ from this version.

HepG2 culture and immunofluorescence double staining were performed in accordance with previous procedure with slight modifications (Jiang et al. 2019). Briefly, HepG2 cells (from ATCC) were maintained in DMEM containing 10% FBS and 100 U penicillin/streptomycin. 1×10^4 cells were seeded into glass bottom cell culture dish followed by DMSO or 100 μM Dex treatment for 6 h. Then cells were fixed in 4% paraformaldehyde for 30 min and 0.5% triton X-100 for 10 min. After blocked by 10% goat serum for 1 hour and incubated with rabbit polyclonal anti-PXR and mouse monoclonal anti-YAP antibodies overnight at 4°C, the cells were stained with fluorescent secondary antibodies including anti-rabbit IgG Alexa Fluor 647 and anti-mouse IgG Alexa Fluor 488 for 1 hour away from light. Nuclei were counterstained with 4′,6-diamidino-2-phenylindole (DAPI). Images were captured by a confocal microscope (Olympus FV3000, Japan). And the immunofluorescence double staining of PXR and YAP was quantified by Image J software.

RNA Isolation and qRT-PCR analysis.

RNA isolation and qRT-PCR analysis of hepatic mRNA expression was performed as described in our previous study (Guan et al. 2019). Mouse *Gapdh* mRNA was used to normalize total RNA levels. The specific primer sequences were designed by Primer Bank and listed in Table S1.

Protein Extraction and Western Blot analysis.

DMD Fast Forward. Published on June 19, 2020 as DOI: 10.1124/dmd.120.000061
This article has not been copyedited and formatted. The final version may differ from this version.

Liver total and nuclear/cytosol protein extracts were prepared as described previously, as well as the conduction of western blot (Jiang et al. 2019). Briefly, 40 μg of protein lysate from liver samples of different groups were used. After separated by 10% SDS-PAGE gel, the protein was transferred onto PVDF membranes (0.45 μm, GE Healthcare Life Sciences, Piscataway, NJ). Blots were blocked in 5% skim milk or 5% BSA followed by incubation with appropriate primary antibodies overnight at 4°C. The detection of specific protein bands and the analysis of the intensity was conducted by an electro-chemiluminescence (ECL) detection kit (GE Healthcare Life Sciences, Piscataway, NJ) and Quantity One software, respectively.

Liquid Chromatography/Mass Spectrometry (LC/MS) and Lipidomic analysis.

Liver lipids were extracted according to a previous method (Li et al. 2018). In short, 20 mg of liver samples were homogenized with PBS and lipids were extracted by 1.2 mL of cold methanol/methyl-tert-butyl ether/H_2O (4:5:5, v/v/v). After being vortexed thoroughly and centrifuged, the upper supernatant of the mixture was transferred into a clean tube and dried in a vacuum oven. The extracts were resuspended in 1 mL mixture of methanol/isopropanol (1:1, v/v) and centrifuged followed by 100 μL upper supernatant added into the injection bottle for further ultra-high-performance liquid chromatography coupled with electrospray ionization high-resolution mass spectrometry (UHPLC-ESI-HRMS) analysis. The chromatographic separation system and MS analysis were similar with the conditions we reported before (Li et al. 2018). Briefly, the sample was analyzed by Ultimate 3000 UPLC system (Dionex Corporation,

DMD Fast Forward. Published on June 19, 2020 as DOI: 10.1124/dmd.120.000061
This article has not been copyedited and formatted. The final version may differ from this version.

Sunnyvale, California). Chromatographic separation was performed on an Ascentis Express C18 2.7 µm column (100 mm × 2.1 mm, Sigma-Aldrich, St. Louis, MO, United States) with gradient elution of 50% acetonitrile (v/v in water with 5 mM ammonium formate and 0.1% formic acid) and 95% isopropanol (v/v in acetonitrile with 5 mM ammonium formate and 0.1% formic acid) at a flow rate of 0.3 mL/min. Mass spectrometry was performed under electrospray positive (ESI+) and negative (ESI−) ionization modes. The main parameters for MS/MS were the same to our previous report (Fu et al. 2019). Lipidomic data were processed using Lipid Search software (Thermo Scientific, San Jose, CA, United States). The structure of lipids was analyzed by comparing accurate mass number and characteristic fragment ion information with the database of the mass spectrum of lipids. The preprocessed data were exported into SIMCA 13.0 software (Umetrics, Kinnelon, NJ, United States) followed by data analysis using principal component analysis (PCA) and orthogonal partial least squares discriminant analysis (OPLS-DA).

Statistical analysis.

Each group consisted at least five animals. All experimental data are presented as the means of ± SD. SPSS19.0 was used for statistical analysis and GraphPad Prism 6.0 was used for graph preparation. Two-tailed Student's test or nonparametric Mann-Whitney U-test was used to assess the differences between groups. Statistical significance is represented as: $^{*}p < 0.05$, $^{**}p < 0.01$, $^{***}p < 0.001$, $^{****}p < 0.0001$.

DMD Fast Forward. Published on June 19, 2020 as DOI: 10.1124/dmd.120.000061
This article has not been copyedited and formatted. The final version may differ from this version.

Results

Dex induces liver enlargement

A recent study revealed that Dex significantly induced liver enlargement, but the underlying details remain unknown (Jiang et al. 2019). After intraperitoneal injection of 0.1 mL/10 g of corn oil or 50 mg/kg of Dex for 5 days (Figure 1A), the liver-to-body-weight ratio was increased from 4.80 ± 0.63% to 6.14 ± 0.53% in the Dex group, which was a significant rise of 27.92% compared to that of the vehicle-treated group (Figure 1B, C). The size of hepatocytes was measured by CTNNB1 staining. A remarkable increase was seen in cell size around the CV area after treatment with Dex (Figure 1D). Quantitative analysis suggested that the size of hepatocytes rose from 721.74 ± 12.75 μm to 894.05 ± 97.66 μm (Figure 1E). There was no significant difference in hepatocyte size around the PV area (Figure S1A, B). These results indicated that Dex (50 mg/kg) promoted hepatomegaly accompanied with hepatocyte enlargement.

Dex is a PXR agonist

Given that PXR activation was reported to induce liver enlargement and high dose of Dex can activate PXR (Staudinger et al. 2001), whether Dex-induced hepatomegaly is related to PXR activation needs to be explored. We first measured the effect of Dex on PXR downstream genes. The protein levels of CYP3A11, CYP2B10 and OATP2 (also known as SLCO1A4 and SLC21A5 in mouse) were significantly increased after treatment with Dex (Figure 2A, B),

DMD Fast Forward. Published on June 19, 2020 as DOI: 10.1124/dmd.120.000061
This article has not been copyedited and formatted. The final version may differ from this version.

suggesting activation of PXR by Dex. Furthermore, the dual-luciferase reporter gene assays were applied to investigate whether human PXR (hPXR) could be transactivated by Dex. In response to positive control RIF, a classic hPXR agonist, luciferase activity of the hPXR-PXRE-luciferase reporter gene assay was markedly increased to 2.74 fold compared with that of the DMSO-treated group, whereas Dex enhanced hPXR reporter gene luciferase activity to 1.45 fold at micromolar concentrations (up to 100 μM) without cellular toxicity (Figure 2C; Figure S2). Taken together, these results indicated that Dex was able to transactivate hPXR and modulate downstream gene of mouse PXR (mPXR), suggesting that Dex is a PXR agonist.

Dex upregulates YAP expression via PXR activation

The YAP signaling pathway plays a vital role in controlling organ size (Tordjmann 2011). Recently, we revealed that YAP is involved in the PXR-induced liver enlargement and there is a potential interaction between PXR and YAP (Jiang et al. 2019). In the current study we determined whether the hepatic YAP pathway contributed to Dex-induced hepatomegaly. Western blot results showed that the protein level of phosphorylated YAP (p-YAP) was decreased to 71.18% of the vehicle group, while the protein level of total YAP and nuclear YAP were increased to 1.44 and 1.40 times of the vehicle group, respectively. This indicated that the increased level of YAP was not only due to nuclear translocation but also due to the up-regulation of total YAP (Figure 3A, B). To further confirm the effect of Dex on the activation of YAP pathway, protein expression of YAP-targeted genes was measured. Protein levels of

DMD Fast Forward. Published on June 19, 2020 as DOI: 10.1124/dmd.120.000061
This article has not been copyedited and formatted. The final version may differ from this version.

ankyrin repeat domain 1 (ANKRD1) and connective tissue growth factor (CTGF) were significantly increased, while cysteine-rich angiogenic inducer 61 (CYR61) expression was unchanged compared to that of the vehicle-treated group (Figure 3C, D). Next, to identify whether PXR and YAP translocated to nucleus together after Dex treatment, immunofluorescence double staining was performed in HepG2 cells. After Dex treatment, the contents of PXR and YAP were significantly increased in the nucleus of HepG2 cells, indicating that Dex induced PXR and YAP nuclear translocation (Figure 3E, F). These data support the hypothesis that Dex, as a PXR activator, could promote YAP nuclear translocation, activate the YAP pathway and then upregulate its downstream target genes.

Dex inhibits hepatocyte proliferation partially due to its anti-inflammation effect.

Hyper-activation of YAP can provoke the proliferation of hepatocytes by upregulating proliferation-related protein (Patel et al. 2017). Moreover, liver enlargement is partially due to the proliferation of hepatocytes (Maronpot et al. 2010). To determine whether hepatocyte proliferation was involved in Dex-induced liver enlargement, the marker of cell proliferation Ki67 was analyzed in liver samples by immunohistochemistry (IHC). There was no visible Ki67 positive cells in either the vehicle-treated group or the Dex-treated group around the CV and portal vein (PV) areas (Figure 4A), while a reduced number of proliferating cell nuclear antigen (PCNA, another cellular proliferation marker) positive cells were observed in livers of mice treated with Dex (Figure 4B), indicating that Dex could not promote hepatocyte proliferation and

DMD Fast Forward. Published on June 19, 2020 as DOI: 10.1124/dmd.120.000061
This article has not been copyedited and formatted. The final version may differ from this version.

hepatocyte proliferation may be not involved in Dex-induced liver enlargement. To examine whether Dex attenuated the proliferative response, protein levels of proliferation-related proteins were measured. The expression of cyclin D1 (CCND1) and PCNA protein was decreased markedly, however, cyclin A1 (CCNA1), cyclin E1 (CCNE1) were unchanged compared to those of the vehicle-treated group (Figure 4C, D), suggesting that the cell cycle was impaired. Gene and protein expression of other regulators involved in cell proliferation such as mesenchymal-epithelial transition factor (MET), epidermal growth factor receptor (EGFR), CTNNB1, c-MYC and FOXM1 protein were also measured to determine potential signals involved in Dex-induced hepatomegaly. As expected, EGFR, c-MYC and FOXM1 were significantly lower than that of the vehicle-treated group both at the mRNA and protein levels, while the expression of CTNNB1 and MET remained unchanged (Figure 4E, F; Figure S3).

Next, the possible mechanism of the Dex-induced inhibition of hepatocyte proliferation was investigated. Previous studies showed the importance of inflammation factors such as tumor necrosis factor (TNF) α and interleukin 6 (IL6) on the regulation of liver growth both in the acute phase and normal status, suggesting that inflammatory factors and cytokines play important roles in hepatocyte proliferation (Han et al. 2018; Nagy et al. 1998; Zimmers et al. 2003). Considering the therapeutic effect of Dex as an anti-inflammation drug, we further measured the expression of inflammation factors. Dex treatment suppressed the mRNA expression level of inflammation factors including *Il6, Tnfa* and interferon γ (*Ifng*), indicating that Dex abrogated hepatocyte proliferation in part by suppressing the production of inflammatory factors (Figure 4G).

DMD Fast Forward. Published on June 19, 2020 as DOI: 10.1124/dmd.120.000061
This article has not been copyedited and formatted. The final version may differ from this version.

Overall, hepatocyte proliferation did not significantly contribute to the Dex-induced hepatomegaly. Dex may counteract the PXR/YAP-induced hepatocyte proliferation partially by the suppression of inflammatory factors.

Dex-induced liver enlargement is involved with lipid accumulation

Dex was previously shown to influence the metabolism of hepatic lipids (Harasim-Symbor et al. 2016). On the other hand, the enlargement of liver and hepatocytes need energy supplied by lipid metabolism. Therefore, we further evaluated the effect of Dex on the liver lipid homeostasis. Prominent microvesicular and macrovesicular fatty changes were observed clearly in the H&E-stained livers in Dex-treated mice (Figure 5A). Oil red O staining further confirmed that the abundance of neutral lipid droplets, stained in red and orange, accumulated in the cytoplasm of hepatocytes after Dex treatment (Figure 5B). Dex significantly increased the levels of TG contents approximately 9 fold higher than that of the vehicle-treated group from 0.04 mmol/g protein to 0.34 mmol/g protein (Figure S4), suggesting that accumulation of lipids may contribute to the increase in liver weight.

To evaluate the effect of Dex on lipid profiles in liver, lipidomic analysis was performed on liver samples. A noticeable separation was found in the principal component analysis (PCA) scatter plots acquired from both positive (Figure 5C) and negative (Figure 5D) ion modes, implicating distinct discrimination in lipid profiles between the vehicle-treated and Dex-treated groups. LipidResearch software and OPLS-DA score plot (Figure 5E, F) were performed to

DMD Fast Forward. Published on June 19, 2020 as DOI: 10.1124/dmd.120.000061
This article has not been copyedited and formatted. The final version may differ from this version.

identify altered lipids in two groups from the database of the mass spectrum of lipids. Lipids that variable importance in projection (VIP) values > 1 were highlighted with red diamonds in the S-plots (Figure 5G, H). Upon the false discovery rate (FDR) test, four lipid species with $p < 0.05$ were selected (Figure 5I-M). Among these classes of lipids, the robustly rising trends of TGs were similar in this specific species no matter composed of unsaturated/saturated fatty acids or different lengths of fatty acids (Figure 5I-J), consistent with the biochemical results mentioned above. However, the trend changes of the other three lipids in liver samples varied even in the same species. Six lipids were reduced and two were upregulated in phosphatidyl ethanolamine (PE) after treatment with Dex (Figure 5K). Eleven phosphatidylcholine (PC) species were decreased and one was increased (Figure 5L). Among the species of phosphatidylinositol (PI), four lipids were altered markedly, two of which were increased and two were downregulated (Figure 5M). Additionally, the hepatic mRNA levels of TGs metabolism-related genes were measured (Figure 5N). Expression of diacylglycerol acyltransferase *Dgat1 and Dgat2* mRNAs encoding regulators of the final step of TGs synthesis, were unchanged while a notable reduction was observed on the mRNAs encoding hormone-sensitive lipase (*Hsl* also known as *Lipe*). There was a downward trend in adipose triglyceride lipase *Atgl* (also known as *Pnpla2*) mRNA but with no significance. Besides, expression of the fatty acid transporter CD36 encoding *Cd36* mRNA was increased markedly, suggesting a larger flux of exogenous fatty acids. At the same time, a reduction was observed on the mRNA level of *Ppara*, which is responsible for the regulation of peroxisomal and mitochondrial fatty acid β-oxidation. Taken together, lipolysis and

DMD Fast Forward. Published on June 19, 2020 as DOI: 10.1124/dmd.120.000061
This article has not been copyedited and formatted. The final version may differ from this version.

fatty acid β-oxidation were suppressed, while the uptake of fatty acids was enhanced, which ultimately contributed to the accumulation of TG. In short, lipidomics and gene analysis suggested that Dex had significant influence on the hepatic lipid metabolism in mice, with much more TGs accumulating in the liver and may eventually lead to liver enlargement.

These data together indicated that Dex significantly enlarged hepatocytes by TG accumulation and then resulted in hepatomegaly.

DMD Fast Forward. Published on June 19, 2020 as DOI: 10.1124/dmd.120.000061
This article has not been copyedited and formatted. The final version may differ from this version.

Discussion

Liver enlargement (hepatomegaly) is characterized by an increased weight or/and size of the liver. It was reported that high-dose Dex treatment of three children induced significant hepatomegaly (Verrips et al. 1998). A similar phenomenon was observed in other clinical steroids treatment cases, as well as in rodents (Iancu et al. 1986; Micuda et al. 2007; Thatcher and Caldwell 1994). Consistently, in the current study the liver was significantly enlarged after intraperitoneally (*i.p.*) dosing of Dex at 50 mg/kg. The increased liver weight was manifested with enlarged hepatocytes around the CV area and obvious fat vacuoles in the liver tissue. Dex induced hepatocyte enlargement around CV area, but there was no significant difference in the size of hepatocytes around PV area. Under physiological conditions, a higher rate of fatty acid oxidation was found in the PV area, and more lipid synthesis in the CV area (Hijmans et al. 2014; Katz et al. 1983), suggesting that Dex-induced hepatomegaly may be related to the lipid accumulation.

Hepatomegaly and hepatocyte hypertrophy are often attributed to the change of cellular contents, including glycogen excess, water retention and lipids accumulation (Maronpot et al. 2010). The current study revealed the increase in intracellular mass, especially lipids, plays important role in Dex-induced hepatomegaly. Lipidomics further revealed alterations in specific altered lipids. Increased TGs were found to account for the majority of lipid changes, which were confirmed by biochemical analysis and histochemical staining. TG metabolism in the liver is

DMD Fast Forward. Published on June 19, 2020 as DOI: 10.1124/dmd.120.000061
This article has not been copyedited and formatted. The final version may differ from this version.

regulated by multiple metabolic enzymes, transporters and transcriptional factors. DGAT1 and DGAT2, catalytic enzymes for the acylation of diacylglycerol (DG) which are the final step of TGs synthesis (Coleman and Lee 2004), were found unchanged at the mRNA level, indicating the synthesis of TGs was not affected by Dex. PNPLA2 regulates TG lipolysis in the adipose tissue, and the resulting DG molecules are then hydrolyzed by LIPE to release monoglycerides (MG) (Alves-Bezerra and Cohen 2017). As expected, gene expression of *Lipe* was reduced, indicating that the lipolysis was inhibited. Combined with the decreased *Ppara* and increased *Cd36* mRNA that regulate fatty acids β-oxidation (Aoyama et al. 1998) and the fatty acids uptake respectively (Buque et al. 2010), these results indicated that lipolysis and β-oxidation were suppressed, while the uptake of fatty acids was enhanced, which ultimately contributed to the accumulation of TGs. Similar results were found in a previous report (Lemke et al. 2008), which uncovered the role of GR-hairy enhancer of split 1 (Hes-1) axis in the regulation of Dex-induced hepatic lipid accumulation. Several other signaling pathways were revealed recently. Notably, MAP kinase phosphatase3 (MKP-3) was confirmed to be the downstream gene of forkhead box protein (FOX) O1 and partially mediated the lipid accumulation by Dex (Feng et al. 2014). miR-17-5p, as a regulator of PPARα, was found to attenuate Dex-induced excessive lipids (Du et al. 2015).

Although Dex is a classic ligand of GR and a vital regulator of the homeostasis of glucose and lipids, the effect of Dex on other nuclear receptors should not be ignored. For example, Dex activates PXR under certain conditions. PXR activation by PCN could lead to significant liver

DMD Fast Forward. Published on June 19, 2020 as DOI: 10.1124/dmd.120.000061
This article has not been copyedited and formatted. The final version may differ from this version.

enlargement. A recent report noted that Dex-induced liver enlargement was related to activation of PXR signaling (Wang et al. 2018). As the crucial regulator for xenobiotic metabolism, PXR modulates the expression of a series of drug metabolizing enzymes and transporters such as CYP3A11, CYP2B10 and OATP2 (also known as SLCO1B1, LST1, OATP-C and SLC21A6 in human, and known as SLCO1A4 and SLC21A5 in mouse) (Hartley et al. 2004; Kliewer 2003; Wang et al. 2003). In human hepatocytes, nanomolar of Dex was found to enhance the expression of *CYP3A4*, a human homolog of the mouse *Cyp3a11* gene, by activation of PXR, whereas Dex could activate PXR under micromolar concentrations (Pascussi et al. 2000). *In vivo* studies also showed that Dex could activate PXR at a higher dose more than 10 mg/kg (Hunter et al. 2017). In the current study, PXR activation by Dex was identified by the increased protein expression of PXR-targeted genes such as *Cyp3a11*, *Cyp2b10* and *Oatp2* (also known as *Slco1a4*, *Oatp1a4* and *Slc21a5* in mouse) *in vivo*. Dex was able to activate hPXR *in vitro* as well. These data together demonstrated that Dex indeed is a PXR agonist in both mice and humans. Furthermore, PXR was activated under the indicated dosage in the animal experiments, consistent with previous reports (Scheer et al. 2010; Schuetz et al. 2000). PXR also plays a crucial role in sustaining the homeostasis of endobiotics such as lipids, and recent studies have investigated the effects of PXR on the regulation of nonalcoholic fatty liver disease (NAFLD) (Cave et al. 2007). PXR can directly bind to FOXA2 to prevent its binding with the promoters of carnitine palmitoyltransferase 1A (CPT1A) and mitochondrial 3-hydroxy-3-methylglutarate-CoA synthase 2 (HMGCS2), and thereby inhibiting fatty acid β oxidation and ketogenesis (Nakamura

DMD Fast Forward. Published on June 19, 2020 as DOI: 10.1124/dmd.120.000061
This article has not been copyedited and formatted. The final version may differ from this version.

et al. 2007). In addition, CD36 was confirmed to be induced by PXR and positively related to increased fatty acids uptake and TG accumulation in the liver (Zhou et al. 2006), implicating a possible role of PXR in the Dex-induced TG accumulation during liver enlargement. Furthermore, YAP has been recently reported to accelerate lipid accumulation (Jeong et al. 2018; Liu et al. 2019) and promote the development and progression of NAFLD with interaction of TGF-β signaling pathways (Chen et al. 2018) *in vivo*, suggesting the close relationship between lipid accumulation and the PXR/YAP activation.

YAP is the critical regulator of liver size. With over-expression of hepatic YAP, the size of liver can be promoted to approaching 4-5 fold than its normal size (Dong et al. 2007). Recently, the contribution of YAP signaling in PXR-induced liver enlargement was uncovered (Jiang et al. 2019). Since PXR was activated by Dex in the current study, YAP signaling may be involved in Dex-induced hepatomegaly. The up-regulation of total YAP, nuclear YAP and YAP downstream proteins together confirmed that YAP signaling was activated in response to Dex treatment and Dex-induced PXR activation. YAP activation was also proven to suppress the expression of gluconeogenic promoted by administration of glucocorticoids such as Dex (Hu et al. 2017). In the present study, excessive glucose may increase the activation of YAP signaling, which ultimately attenuated the Dex-induced flux of glucose. PXR and YAP were found to translocate to the HepG2 cell nucleus 6 h after the Dex treatment, which was consistent with our previous finding and suggested a potential interaction between PXR and YAP (Jiang et al. 2019).

DMD Fast Forward. Published on June 19, 2020 as DOI: 10.1124/dmd.120.000061
This article has not been copyedited and formatted. The final version may differ from this version.

Interestingly, the best time point to observe this co-localization was 6 h after Dex treatment instead of 48 h.

YAP activation could evoke cell proliferation, which is also thought to be involved in the PXR-induced liver enlargement (Huang et al. 2005). Intriguingly, the present results showed a different trend after Dex treatment. The staining of proliferation markers Ki67 and PCNA revealed no induction of proliferation around the CV and PV areas by Dex. The down-regulation of CCND1, a member of cyclins, controls the entry of cell cycle, suggested that DNA synthesis and mitosis of hepatic cells was inhibited. The markable reduction of CCND1 and PCNA have revealed that proliferation response was arrested. Several proliferation-related factors were further assessed. Wnt/β-catenin signaling is another vital pathway which regulates organ size, and it is considered to be evidently activated by YAP activation (Camargo et al. 2007). However, no difference was noted between vehicle- and Dex-treated mice in the expression of CTNNB1, which may involve the interplay of Hippo/Wnt signaling. Receptor tyrosine kinases (RTKs) including MET and EGFR, as the upstream regulators of cyclins including CCND1, was found to partially mediate hepatocyte proliferation (Bhushan et al. 2019). c-MYC was also reported to be the regulator of hepatocyte proliferation (Baena et al. 2005). Consistently, a reduction was both observed in the protein and mRNA level of c-MYC in Dex-treated mice. Additionally, FOXM1, as the downstream targeted gene of MET, EGFR and c-MYC, is one of the major transcription factors that controls the cell cycle including progression to S-phase and mitosis (Blanco-Bose et al. 2008; Francica et al. 2016; Stoll et al. 2016). In the present study, decreased EGFR, c-MYC,

DMD Fast Forward. Published on June 19, 2020 as DOI: 10.1124/dmd.120.000061
This article has not been copyedited and formatted. The final version may differ from this version.

and FOXM1 indicated their possible roles in the impaired cell cycle and proliferation inhibition by Dex. Inflammatory factors such as interleukin 6 (IL6) were capable of rescuing the inhibition of hepatocyte proliferation by Dex in the acute phase (Han et al. 2018) and induce hepatomegaly by continuous administration in physical stasis (Zimmers et al. 2003). Considering the potency of the anti-inflammatory effect of Dex, we hypothesized that YAP signaling promoted proliferation was partially counteracted by Dex-induced anti-inflammatory effect. Here, Dex treatment suppressed mRNA expression level of inflammation factors including *Il6*, *Tnfa* and interferon γ (*Ifng*), indicating that Dex abrogated hepatocyte proliferation in part by suppressing the production of inflammatory factors. These data together demonstrated that Dex-induced liver enlargement is mainly caused by liver cell enlargement instead of hepatocyte proliferation and Dex may counteract the YAP-induced–hepatocyte proliferation partially by the suppression of inflammation factors

In summary, the current study demonstrated that Dex, at a high dose used to treat inflammatory diseases, can induce liver cell enlargement and hepatomegaly possibly by activating PXR and then inducing nuclear translocation of YAP and activating YAP signaling. Though it has been proven that PXR-induced liver enlargement is YAP-dependent (Jiang et al. 2019), whether Dex-induced hepatomegaly is PXR-dependent still needs to be confirmed using PXR lost-of-function models such as *Pxr* knockout mice. Furthermore, Dex-induced hepatomegaly was not due to hepatocyte proliferation likely due to its anti-inflammation effect of suppression of inflammation factors. The Dex-induced hepatocyte enlargement was mostly

DMD Fast Forward. Published on June 19, 2020 as DOI: 10.1124/dmd.120.000061
This article has not been copyedited and formatted. The final version may differ from this version.

attributable to the accumulation of lipids such as triglycerides. These findings provide new insights for understanding the mechanism of Dex-induced hepatomegaly and provide more information on its clinical use in the future.

Authorship Contributions

Participated in research design: Bi, Jiao, Huang

Conducted experiments: Jiao, Yao, Zhao, Zhou, Gao, Fan, Chen, Li, Jiang, Yang

Performed data analysis: Jiao, Yao

Wrote or contributed to the writing of the manuscript: Jiao, Bi, Gonzalez

DMD Fast Forward. Published on June 19, 2020 as DOI: 10.1124/dmd.120.000061
This article has not been copyedited and formatted. The final version may differ from this version.

References

Alves-Bezerra M and Cohen DE (2017) Triglyceride Metabolism in the Liver. *Compr Physiol* **8:** 1-8

Aoyama T, Peters JM, Iritani N, Nakajima T, Furihata K, Hashimoto T and Gonzalez FJ (1998) Altered constitutive expression of fatty acid-metabolizing enzymes in mice lacking the peroxisome proliferator-activated receptor alpha (PPARalpha). *J Biol Chem* **273:** 5678-5684

Baena E, Gandarillas A, Vallespinós M, Zanet J, Bachs O, Redondo C, Fabregat I, Martinez-A C and de Alborán IM (2005) c-Myc regulates cell size and ploidy but is not essential for postnatal proliferation in liver. *Proc Natl Acad Sci U S A* **102:** 7286-7291

Bhushan B, Stoops JW, Mars WM, Orr A, Bowen WC, Paranjpe S and Michalopoulos GK (2019) TCPOBOP-Induced Hepatomegaly and Hepatocyte Proliferation are Attenuated by Combined Disruption of MET and EGFR Signaling. *Hepatology* **69:** 1702-1718

Blanco-Bose WE, Murphy MJ, Ehninger A, Offner S, Dubey C, Huang W, Moore DD and Trumpp A (2008) C-Myc and its target FoxM1 are critical downstream effectors of constitutive androstane receptor (CAR) mediated direct liver hyperplasia. *Hepatology* **48:** 1302-1311

Botts S, Ennulat D, Francke-Carroll S, Graham M, Maronpot RR and Mohutsky M (2010) Introduction to Hepatic Drug Metabolizing Enzyme Induction in Drug Safety Evaluation Studies. *Toxicol Pathol* **38:** 796-798

Buckley DB and Klaassen CD (2009) Induction of mouse UDP-glucuronosyltransferase mRNA expression in liver and intestine by activators of aryl-hydrocarbon receptor, constitutive

androstane receptor, pregnane X receptor, peroxisome proliferator-activated receptor alpha, and nuclear factor erythroid 2-related factor 2. *Drug Metab Dispos* **37:** 847-856

Buque X, Martinez MJ, Cano A, Miquilena-Colina ME, Garcia-Monzon C, Aspichueta P and Ochoa B (2010) A subset of dysregulated metabolic and survival genes is associated with severity of hepatic steatosis in obese Zucker rats. *J Lipid Res* **51:** 500-513

Camargo FD, Gokhale S, Johnnidis JB, Fu D, Bell GW, Jaenisch R and Brummelkamp TR (2007) YAP1 increases organ size and expands undifferentiated progenitor cells. *Curr Biol* **17:** 2054-2060

Cave M, Deaciuc I, Mendez C, Song Z, Joshi-Barve S, Barve S and McClain C (2007) Nonalcoholic fatty liver disease: predisposing factors and the role of nutrition. *J Nutr Biochem* **18:** 184-195

Chen P, Luo Q, Huang C, Gao Q, Li L, Chen J, Chen B, Liu W, Zeng W and Chen Z (2018) Pathogenesis of non-alcoholic fatty liver disease mediated by YAP. *Hepatol Int* **12:** 26-36

Cheng X, Maher J, Dieter MZ and Klaassen CD (2005) Regulation of mouse organic anion-transporting polypeptides (Oatps) in liver by prototypical microsomal enzyme inducers that activate distinct transcription factor pathways. *Drug Metab Dispos* **33:** 1276-1282

Coleman RA and Lee DP (2004) Enzymes of triacylglycerol synthesis and their regulation. *Prog Lipid Res* **43:** 134-176

Cui A, Fan H, Zhang Y, Zhang Y, Niu D, Liu S, Liu Q, Ma W, Shen Z, Shen L, Liu Y, Zhang H, Xue Y, Cui Y, Wang Q, Xiao X, Fang F, Yang J, Cui Q and Chang Y (2019)

Dexamethasone-induced Krüppel-like factor 9 expression promotes hepatic gluconeogenesis and hyperglycemia. *J Clin Invest* **129:** 2266-2278

Dong J, Feldmann G, Huang J, Wu S, Zhang N, Comerford SA, Gayyed Mariana F, Anders RA, Maitra A and Pan D (2007) Elucidation of a Universal Size-Control Mechanism in Drosophila and Mammals. *Cell* **130:** 1120-1133

Du WW, Liu F, Shan SW, Ma XC, Gupta S, Jin T, Spaner D, Krylov SN, Zhang Y, Ling W and Yang BB (2015) Inhibition of Dexamethasone-induced Fatty Liver Development by Reducing miR-17-5p Levels. *Mol Ther* **23:** 1222-1233

Ericson-Neilsen W and Kaye AD (2014) Steroids: pharmacology, complications, and practice delivery issues. *Ochsner J* **14:** 203-207

Feng B, He Q and Xu H (2014) FOXO1-dependent up-regulation of MAP kinase phosphatase 3 (MKP-3) mediates glucocorticoid-induced hepatic lipid accumulation in mice. *Mol Cell Endocrinol* **393:** 46-55

Francica P, Nisa L, Aebersold DM, Langer R, Bladt F, Blaukat A, Stroka D, Martínez MR, Zimmer Y and Medová M (2016) Depletion of FOXM1 via MET Targeting Underlies Establishment of a DNA Damage-Induced Senescence Program in Gastric Cancer. *Clin Cancer Res* **22:** 5322-5336

Fu K, Wang C, Gao Y, Fan S, Zhang H, Sun J, Jiang Y, Liu C, Guan L, Liu J, Huang M and Bi H (2019) Metabolomics and Lipidomics Reveal the Effect of Hepatic Vps33b Deficiency on Bile Acids and Lipids Metabolism. *Front Pharmacol* **10:** 276

Glantz A, Marschall HU, Lammert F and Mattsson LA (2005) Intrahepatic cholestasis of pregnancy: a randomized controlled trial comparing dexamethasone and ursodeoxycholic acid. *Hepatology* **42:** 1399-1405

Guan L, Chen Y, Wang Y, Zhang H, Fan S, Gao Y, Jiao T, Fu K, Sun J, Yu A, Huang M and Bi H (2019) Effects of carnitine palmitoyltransferases on cancer cellular senescence. *J Cell Physiol* **234:** 1707-1719

Han R, Zhang F, Wan C, Liu L, Zhong Q and Ding W (2018) Effect of perfluorooctane sulphonate-induced Kupffer cell activation on hepatocyte proliferation through the NF-κB/TNF-α/IL-6-dependent pathway. *Chemosphere* **200:** 283-294

Harasim-Symbor E, Konstantynowicz-Nowicka K and Chabowski A (2016) Additive effects of dexamethasone and palmitate on hepatic lipid accumulation and secretion. *J Mol Endocrinol* **57:** 261-273

Hartley DP, Dai X, He YD, Carlini EJ, Wang B, Huskey SE, Ulrich RG, Rushmore TH, Evers R and Evans DC (2004) Activators of the rat pregnane X receptor differentially modulate hepatic and intestinal gene expression. *Mol Pharmacol* **65:** 1159-1171

Hijmans BS, Grefhorst A, Oosterveer MH and Groen AK (2014) Zonation of glucose and fatty acid metabolism in the liver: mechanism and metabolic consequences. *Biochimie* **96:** 121-129

Hu Y, Shin DJ, Pan H, Lin Z, Dreyfuss JM, Camargo FD, Miao J and Biddinger SB (2017) YAP suppresses gluconeogenic gene expression through PGC1alpha. *Hepatology* **66:** 2029-2041

Huang J, Wu S, Barrera J, Matthews K and Pan D (2005) The Hippo signaling pathway coordinately regulates cell proliferation and apoptosis by inactivating Yorkie, the Drosophila Homolog of YAP. *Cell* **122:** 421-434

Hunter SR, Vonk A, Mullen Grey AK and Riddick DS (2017) Role of Glucocorticoid Receptor and Pregnane X Receptor in Dexamethasone Induction of Rat Hepatic Aryl Hydrocarbon Receptor Nuclear Translocator and NADPH-Cytochrome P450 Oxidoreductase. *Drug Metab Dispos* **45:** 118-129

Iancu TC, Shiloh H and Dembo L (1986) Hepatomegaly following short-term high-dose steroid therapy. *J Pediatr Gastroenterol Nutr* **5:** 41-46

Jeong S-H, Kim H-B, Kim M-C, Lee J-M, Lee JH, Kim J-H, Kim J-W, Park W-Y, Kim S-Y, Kim JB, Kim H, Kim J-M, Choi H-S and Lim D-S (2018) Hippo-mediated suppression of IRS2/AKT signaling prevents hepatic steatosis and liver cancer. *J Clin Invest* **128:** 1010-1025

Jiang Y, Feng D, Ma X, Fan S, Gao Y, Fu K, Wang Y, Sun J, Yao X, Liu C, Zhang H, Xu L, Liu A, Gonzalez FJ, Yang Y, Gao B, Huang M and Bi H (2019) Pregnane X Receptor Regulates Liver Size and Liver Cell Fate by Yes-Associated Protein Activation in Mice. *Hepatology* **69:** 343-358

Katz NR, Fischer W and Giffhorn S (1983) Distribution of enzymes of fatty acid and ketone body metabolism in periportal and perivenous rat-liver tissue. *Eur J Biochem* **135:** 103-107

Kliewer SA (2003) The nuclear pregnane X receptor regulates xenobiotic detoxification. *J Nutr* **133:** 2444S-2447S

Kliewer SA, Goodwin B and Willson TM (2002) The nuclear pregnane X receptor: a key regulator of xenobiotic metabolism. *Endocr Rev* **23:** 687-702

Kliewer SA, Moore JT, Wade L, Staudinger JL, Watson MA, Jones SA, McKee DD, Oliver BB, Willson TM, Zetterstrom RH, Perlmann T and Lehmann JM (1998) An orphan nuclear receptor activated by pregnanes defines a novel steroid signaling pathway. *Cell* **92:** 73-82

Lemke U, Krones-Herzig A, Berriel Diaz M, Narvekar P, Ziegler A, Vegiopoulos A, Cato AC, Bohl S, Klingmuller U, Screaton RA, Muller-Decker K, Kersten S and Herzig S (2008) The glucocorticoid receptor controls hepatic dyslipidemia through Hes1. *Cell Metab* **8:** 212-223

Li J, Gao Y, Guan L, Zhang H, Sun J, Gong X, Li D, Chen P, Ma Z, Liang X, Huang M and Bi H (2018) Discovery of Phosphatidic Acid, Phosphatidylcholine, and Phosphatidylserine as Biomarkers for Early Diagnosis of Endometriosis. *Front Physiol* **9:** 14

Liu Y, Ren H, Zhou Y, Shang L, Zhang Y, Yang F and Shi X (2019) The hypoxia conditioned mesenchymal stem cells promote hepatocellular carcinoma progression through YAP mediated lipogenesis reprogramming. *J Exp Clin Cancer Res* **38:** 228

Maronpot RR, Yoshizawa K, Nyska A, Harada T, Flake G, Mueller G, Singh B and Ward JM (2010) Hepatic Enzyme Induction. *Toxicol Pathol* **38:** 776-795

Micuda S, Fuksa L, Mundlova L, Osterreicher J, Mokry J, Cermanova J, Brcakova E, Staud F, Pokorna P and Martinkova J (2007) Morphological and functional changes in p-glycoprotein during dexamethasone-induced hepatomegaly. *Clin Exp Pharmacol Physiol* **34:** 296-303

Nagy P, Kiss A, Schnur J and Thorgeirsson SS (1998) Dexamethasone inhibits the proliferation of hepatocytes and oval cells but not bile duct cells in rat liver. *Hepatology* **28:** 423-429

Nakamura K, Moore R, Negishi M and Sueyoshi T (2007) Nuclear pregnane X receptor cross-talk with FoxA2 to mediate drug-induced regulation of lipid metabolism in fasting mouse liver. *J Biol Chem* **282:** 9768-9776

Pascussi JM, Drocourt L, Fabre JM, Maurel P and Vilarem MJ (2000) Dexamethasone induces pregnane X receptor and retinoid X receptor-alpha expression in human hepatocytes: synergistic increase of CYP3A4 induction by pregnane X receptor activators. *Mol Pharmacol* **58:** 361-372

Patel SH, Camargo FD and Yimlamai D (2017) Hippo Signaling in the Liver Regulates Organ Size, Cell Fate, and Carcinogenesis. *Gastroenterology* **152:** 533-545

Petta I, Dejager L, Ballegeer M, Lievens S, Tavernier J, De Bosscher K and Libert C (2016) The Interactome of the Glucocorticoid Receptor and Its Influence on the Actions of Glucocorticoids in Combatting Inflammatory and Infectious Diseases. *Microbiol Mol Biol Rev* **80:** 495-522

Rhen T and Cidlowski JA (2005) Antiinflammatory action of glucocorticoids--new mechanisms for old drugs. *N Engl J Med* **353:** 1711-1723

Scheer N, Ross J, Kapelyukh Y, Rode A and Wolf CR (2010) In vivo responses of the human and murine pregnane X receptor to dexamethasone in mice. *Drug Metab Dispos* **38:** 1046-1053

Schuetz EG, Schmid W, Schutz G, Brimer C, Yasuda K, Kamataki T, Bornheim L, Myles K and Cole TJ (2000) The glucocorticoid receptor is essential for induction of cytochrome P-4502B by

steroids but not for drug or steroid induction of CYP3A or P-450 reductase in mouse liver. *Drug Metab Dispos* **28:** 268-278

Staudinger JL, Goodwin B, Jones SA, Hawkins-Brown D, MacKenzie KI, LaTour A, Liu Y, Klaassen CD, Brown KK, Reinhard J, Willson TM, Koller BH and Kliewer SA (2001) The nuclear receptor PXR is a lithocholic acid sensor that protects against liver toxicity. *Proc Natl Acad Sci U S A* **98:** 3369-3374

Stoll SW, Stuart PE, Swindell WR, Tsoi LC, Li B, Gandarillas A, Lambert S, Johnston A, Nair RP and Elder JT (2016) The EGF receptor ligand amphiregulin controls cell division via FoxM1. *Oncogene* **35:** 2075-2086

Thatcher NJ and Caldwell J (1994) Origins of hepatomegaly produced by dexamethasone (DEX), pregnenolone 16 alpha-carbonitrile (PCN) and phenobarbitone (PB) in female Sprague-Dawley rats. *Biochem Soc Trans* **22:** 132S

Tordjmann T (2011) Hippo signalling: liver size regulation and beyond. *Clin Res Hepatol Gastroenterol* **35:** 344-346

Tumaneng K, Schlegelmilch K, Russell RC, Yimlamai D, Basnet H, Mahadevan N, Fitamant J, Bardeesy N, Camargo FD and Guan KL (2012) YAP mediates crosstalk between the Hippo and PI(3)K-TOR pathways by suppressing PTEN via miR-29. *Nat Cell Biol* **14:** 1322-1329

Verrips A, Rotteveel JJ and Lippens R (1998) Dexamethasone-induced hepatomegaly in three children. *Pediatr Neurol* **19:** 388-391

Wang H, Faucette SR, Gilbert D, Jolley SL, Sueyoshi T, Negishi M and LeCluyse EL (2003) Glucocorticoid receptor enhancement of pregnane X receptor-mediated CYP2B6 regulation in primary human hepatocytes. *Drug Metab Dispos* **31:** 620-630

Wang X, Wang F, Lu Z, Jin X and Zhang Y (2018) Semi-quantitative profiling of bile acids in serum and liver reveals the dosage-related effects of dexamethasone on bile acid metabolism in mice. *J Chromatogr B Analyt Technol Biomed Life Sci* **1095:** 65-74

Xie W, Barwick JL, Downes M, Blumberg B, Simon CM, Nelson MC, Neuschwander-Tetri BA, Brunt EM, Guzelian PS and Evans RM (2000) Humanized xenobiotic response in mice expressing nuclear receptor SXR. *Nature* **406:** 435-439

Zeng H, Jiang Y, Chen P, Fan X, Li D, Liu A, Ma X, Xie W, Liu P, Gonzalez FJ, Huang M and Bi H (2017) Schisandrol B protects against cholestatic liver injury through pregnane X receptors. *Br J Pharmacol* **174:** 672-688

Zhou J, Zhai Y, Mu Y, Gong H, Uppal H, Toma D, Ren S, Evans RM and Xie W (2006) A novel pregnane X receptor-mediated and sterol regulatory element-binding protein-independent lipogenic pathway. *J Biol Chem* **281:** 15013-15020

Zimmers TA, McKillop IH, Pierce RH, Yoo JY and Koniaris LG (2003) Massive liver growth in mice induced by systemic interleukin 6 administration. *Hepatology* **38:** 326-334

DMD Fast Forward. Published on June 19, 2020 as DOI: 10.1124/dmd.120.000061
This article has not been copyedited and formatted. The final version may differ from this version.

Footnotes:

Funding information

The work was supported by the Natural Science Foundation of China (Grants: 81973392); the National Key Research and Development Program (Grant: 2017YFE0109900); the Natural Science Foundation of Guangdong (Grant: 2017A030311018); the 111 project (Grant: B16047); the Key Laboratory Foundation of Guangdong Province (Grant: 2017B030314030); the Local Innovative and Research Teams Project of Guangdong Pearl River Talents Program (2017BT01Y093); the National Engineering and Technology Research Center for New drug Druggability Evaluation (Seed Program of Guangdong Province, 2017B090903004); and the Intramural Research Program of the National Institutes of Health National Cancer Institute.

.

DMD Fast Forward. Published on June 19, 2020 as DOI: 10.1124/dmd.120.000061
This article has not been copyedited and formatted. The final version may differ from this version.

Legends for Figures

Figure 1. Dex significantly induces liver enlargement in mice. (A) Mice were intraperitoneally treated with vehicle (corn oil, 0.1 mL/10 g) or Dex (50 mg/kg/d) for 5 days. (B) Liver-to-body-weight ratios. Data are expressed as mean ± SD (n = 5). (C) Representative morphological pictures of mice livers of the vehicle or Dex group. (D) CTNNB1 staining of representative liver samples measuring the size of hepatocytes around the CV area. (E) Quantification of the size of hepatocytes around the CV area. Data are expressed as mean ± SD (n = 3). $^{*}p < 0.05$ compared to the vehicle group.

Figure 2. Dex activates mPXR and hPXR. (A-B) Western blot and quantification of mPXR downstream proteins from vehicle- or Dex-treated mice livers. Data are expressed as mean ± SD (n = 3). $^{*}p < 0.05$, $^{**}p < 0.01$ compared to the vehicle group. (C) Dual-luciferase reporter gene assay was used to determine the effect of RIF or Dex on hPXR activation in HEK293T cells. Data are expressed as mean ± SD (n = 5). $^{**}p< 0.01$, $^{***}p < 0.001$, $^{****}p < 0.0001$ compared to the vehicle group.

Figure 3. Effect of Dex on YAP signaling pathway. (A-B) Western blot analysis and quantification of total YAP, nuclear YAP and cytoplasmic p-YAP protein of liver samples after a

DMD Fast Forward. Published on June 19, 2020 as DOI: 10.1124/dmd.120.000061
This article has not been copyedited and formatted. The final version may differ from this version.

5-day treatment with Dex. (C-D) Western blot analysis and quantification of YAP downstream proteins of liver samples after Dex treatment. Data are expressed as mean ± SD (n = 3). $^{*}p < 0.05$, $^{**}p < 0.01$ compared to the vehicle group. (E) Confocal microscopy displaying PXR and YAP distribution in HepG2 cells treated with 100 μM of Dex for 6 h. Scale bar = 40 μm, (F) Quantification of immunofluorescence double staining of YAP and PXR. Data are expressed as mean ± SD (n = 3). $^{*}p < 0.05$ compared to the vehicle group.

Figure 4. Effect of Dex on hepatocyte proliferation. (A-B) IHC staining of Ki67 and PCNA in mice treated with the vehicle or Dex. (C-F) Western blot analysis and quantification of proliferation-related protein in mice following a 5-day treatment with the vehicle or Dex. Data are expressed as mean ± SD (n = 3). $^{*}p < 0.05$, $^{**}p < 0.01$, $^{****}p < 0.0001$ compared to the vehicle group. (G) qRT-PCR analysis of inflammatory factors in mice in response to the vehicle or Dex treatment. Data are expressed as mean ± SD (n = 5). $^{*}p < 0.05$, $^{***}p < 0.001$ compared to the vehicle group.

Figure 5. Effect of Dex on the lipid profiles and lipid homeostasis. (A) H&E staining of representative liver samples–from the vehicle- or Dex-treated mice. (B) Oil red O staining of representative liver samples of mice treated with the vehicle or Dex. (C-D) PCA scatter plots,

DMD Fast Forward. Published on June 19, 2020 as DOI: 10.1124/dmd.120.000061
This article has not been copyedited and formatted. The final version may differ from this version.

(E-F) OPLS-DA score plots, and (G-H) S-plots under positive and negative ion modes of lipid profiles from livers of mice treated with the vehicle or Dex. For PCA and OPLS-DA plots (C-F), blue diamonds represent the vehicle-treated mice, red diamonds represent the Dex-treated mice and pink diamonds represent the quality controls). For S-plots (G-H), the specific calculated lipid components with p-value less than 0.05, VIP > 1 were highlighted by red diamonds. (I-M) Altered lipid contents and species in liver samples of mice treated with the vehicle or Dex. (I-J) TG; (K) PE; (L) PC; (M) PI. (N) qRT-PCR analysis of TG metabolic genes in mice treated with the vehicle or Dex. Data are expressed as mean ± SD (n = 4 or 5). $^{*}p < 0.05$, $^{**}p < 0.01$, $^{***}p < 0.001$ compared to the vehicle group.

DMD Fast Forward. Published on June 19, 2020 as DOI: 10.1124/dmd.120.000061
This article has not been copyedited and formatted. The final version may differ from this version.

Figure 1

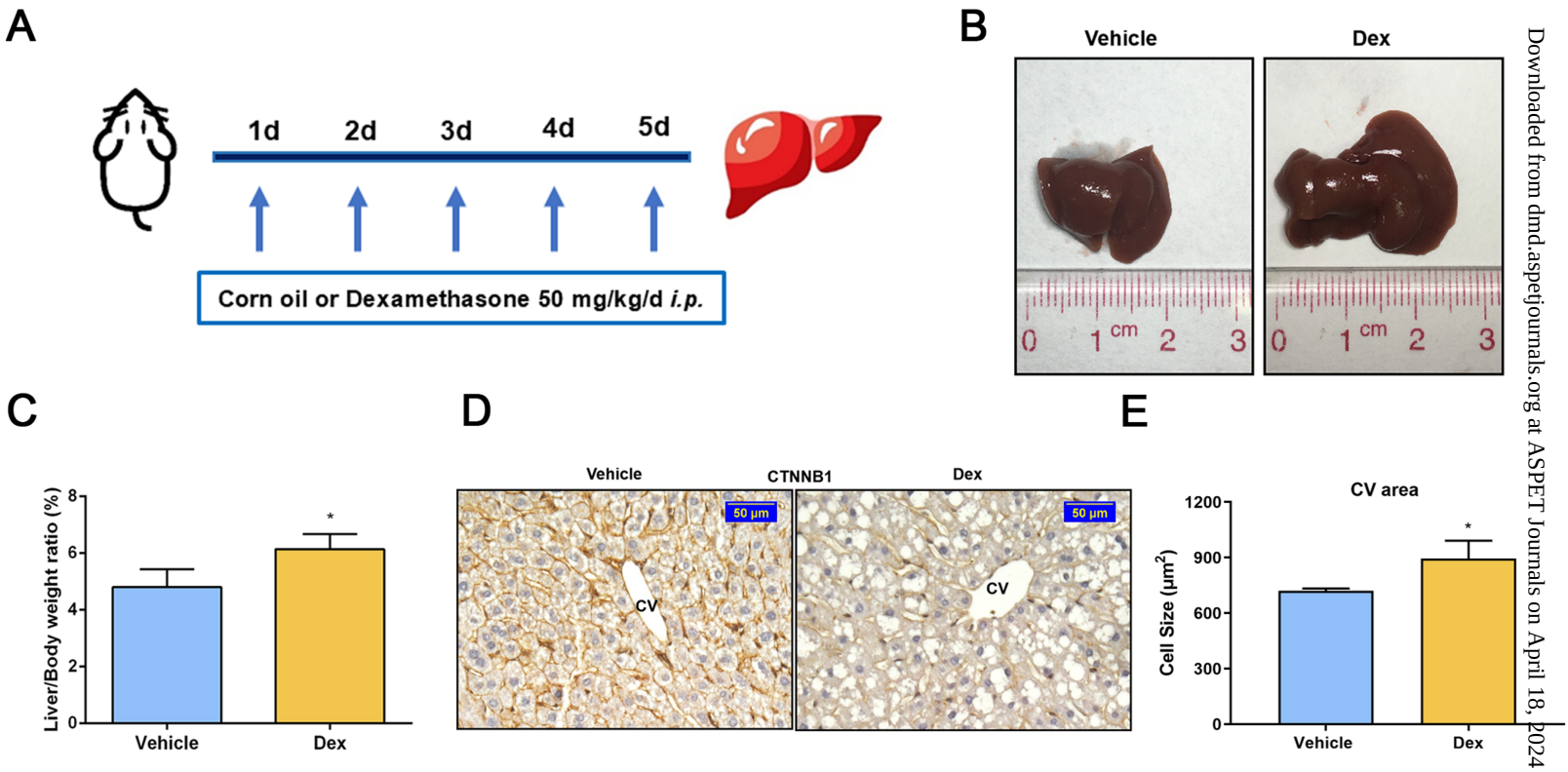

DMD Fast Forward. Published on June 19, 2020 as DOI: 10.1124/dmd.120.000061
This article has not been copyedited and formatted. The final version may differ from this version.

Figure 2

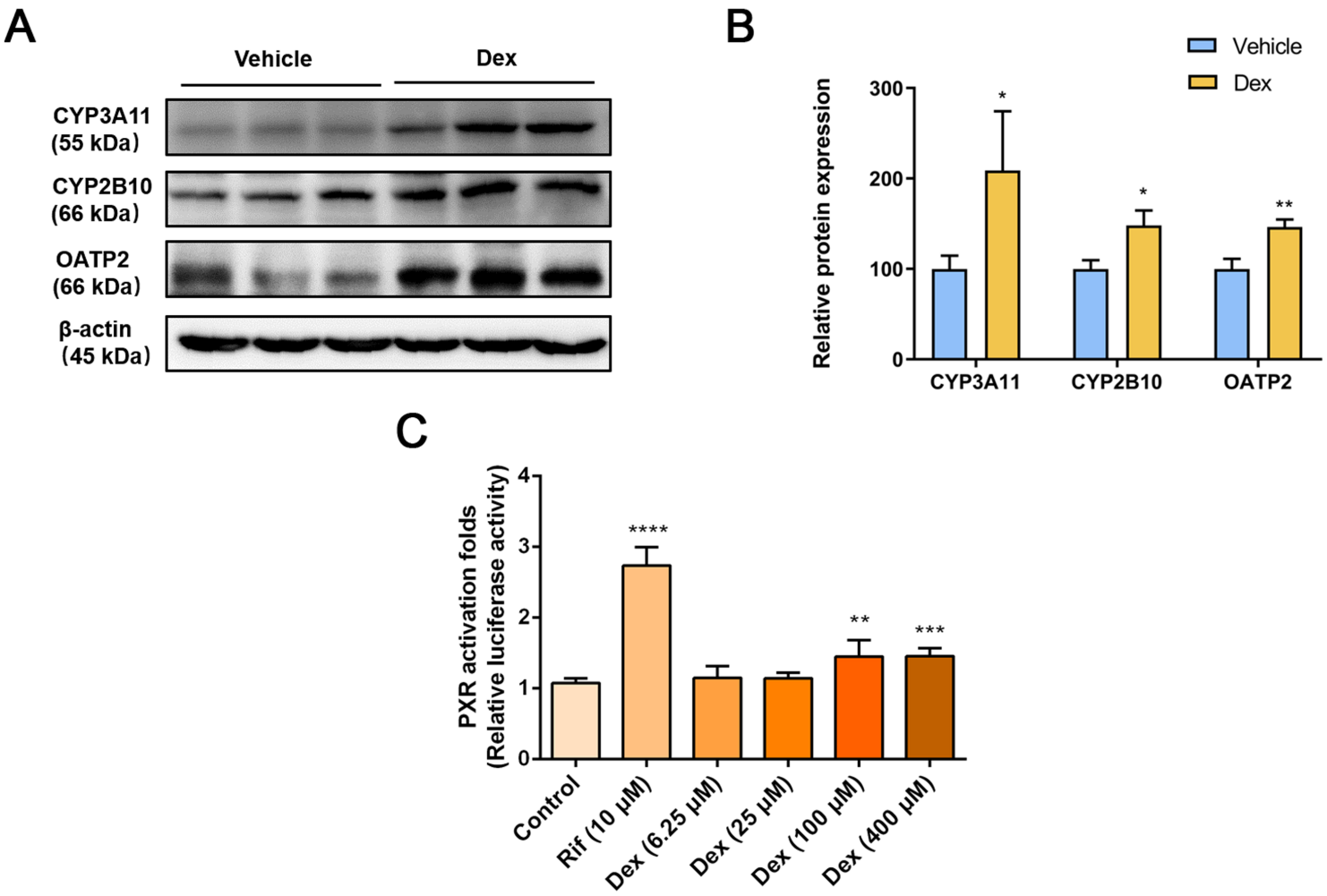

DMD Fast Forward. Published on June 19, 2020 as DOI: 10.1124/dmd.120.000061
This article has not been copyedited and formatted. The final version may differ from this version.

Figure 3

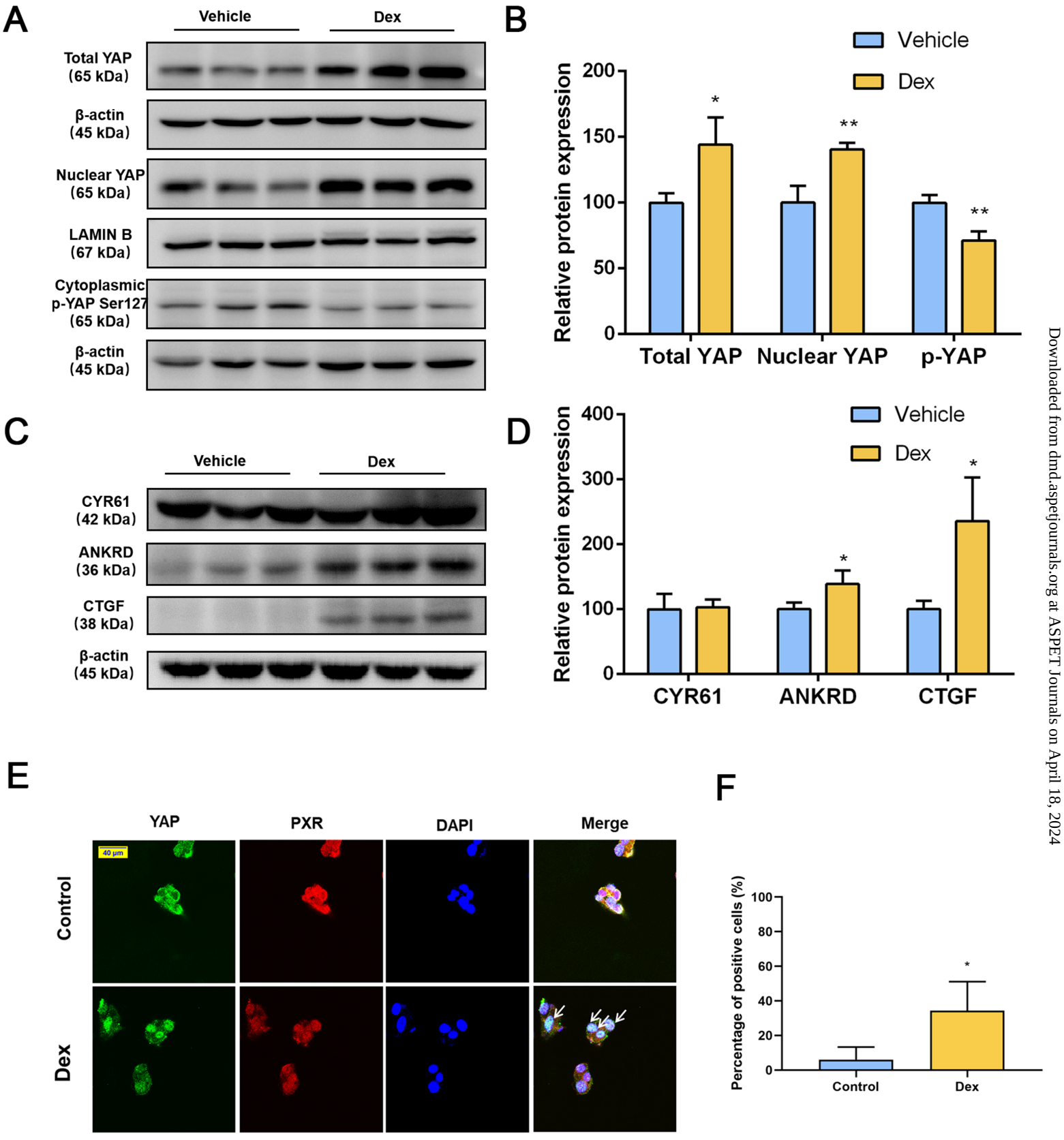

DMD Fast Forward. Published on June 19, 2020 as DOI: 10.1124/dmd.120.000061
This article has not been copyedited and formatted. The final version may differ from this version.

Figure 4

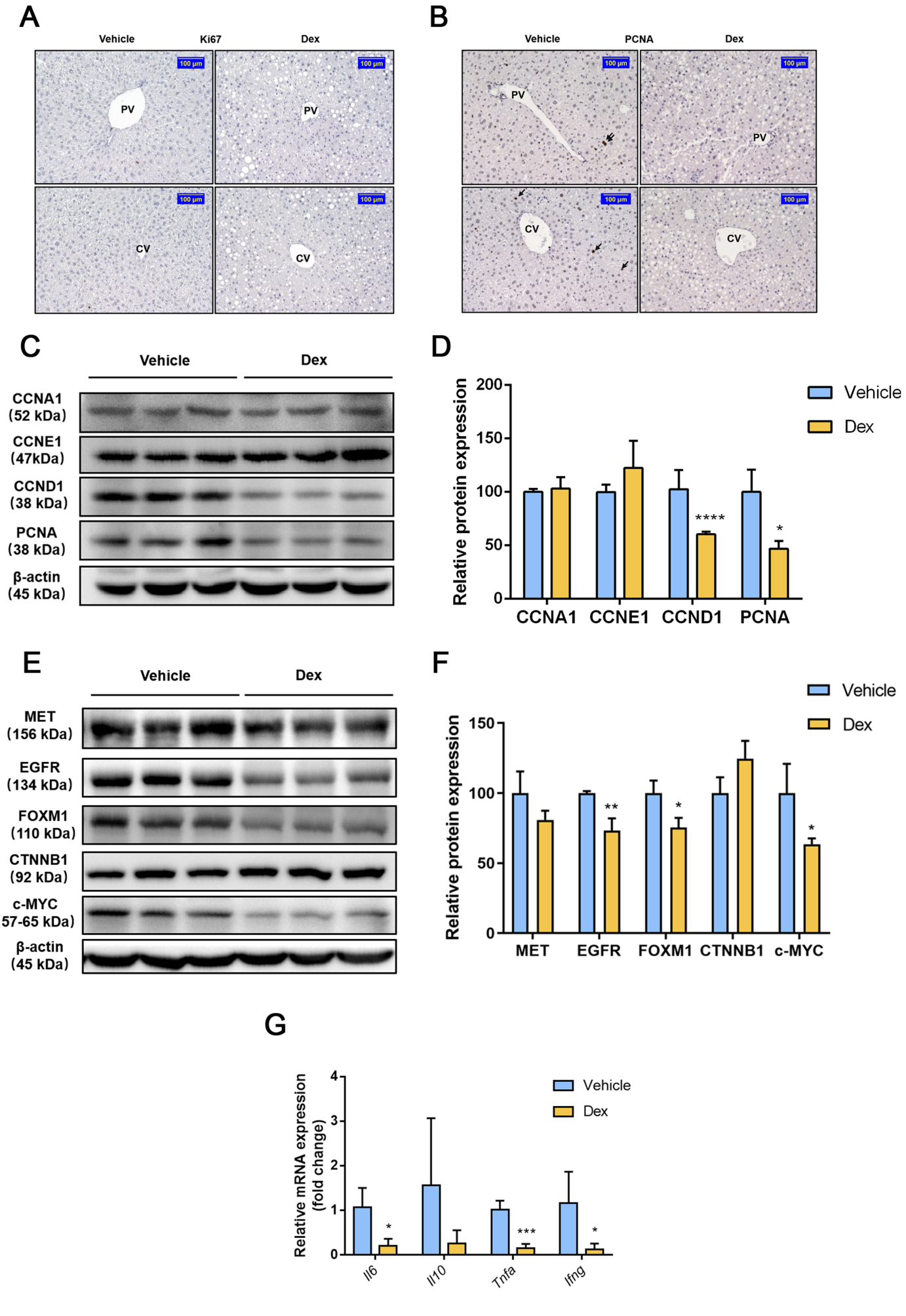

DMD Fast Forward. Published on June 19, 2020 as DOI: 10.1124/dmd.120.000061
This article has not been copyedited and formatted. The final version may differ from this version.

Figure 5